

[³H]Pirenzepine and [³H]Quinuclidinyl Benzilate Binding to Brain Muscarinic Cholinergic Receptors

Differences in Measured Receptor Density Are Not Explained by Differences in Receptor Isomerization

GARY R. LUTHIN¹ AND BARRY B. WOLFE²

Department of Pharmacology/G3, University of Pennsylvania School of Medicine, Philadelphia, Pennsylvania 19104

Received February 1, 1984; Accepted May 16, 1984

SUMMARY

Muscarinic receptor densities were measured in membranes prepared from rat cerebral cortex using [³H]pirenzepine and [³H]quinuclidinyl benzilate. Isotherms of equilibrium binding data modeled to a single apparent binding site for both ligands. However, as has been reported previously, [³H]pirenzepine labeled only a small fraction of the binding sites that were labeled by [³H]quinuclidinyl benzilate. This observation has been used to support the hypothesis that subtypes of muscarinic receptors exist. Several investigators have previously suggested that antagonist binding to muscarinic receptors involves an isomerization of the receptor-antagonist complex, and it is only the isomerized form of the receptor that is identified by radioligand binding studies. To examine the possibility that the difference in the density of binding sites identified by [³H]pirenzepine and [³H]quinuclidinyl benzilate is due to differences in the degree of isomerization of the receptor associated with the binding of each ligand, the kinetics of the binding of [³H]pirenzepine and [³H]quinuclidinyl benzilate to membranes prepared from rat cerebral cortex were examined. The pseudo-first-order rate constant of association for both ligands showed a nonlinear (hyperbolic) dependence on ligand concentration. These results suggested that a rapidly equilibrating initial binding step was followed by a more slowly equilibrating isomerization of the initially formed ligand-receptor complex. The kinetic data were computer-modeled to obtain estimates of the equilibrium constants for both reaction steps. The equilibrium constants for the isomerization step were 0.1 and 0.004 for [³H]pirenzepine and [³H]quinuclidinyl benzilate, respectively. Our measurements, in agreement with others, suggested that only the fraction of receptors which isomerized were measurable using filtration binding assays. Although essentially all (99.6%) of the [³H]quinuclidinyl benzilate binding sites appeared to isomerize, only 90% of the [³H]pirenzepine binding sites isomerized, and thus only 90% were measured in our assay. It therefore appears that differences in receptor isomerization can partially, but not wholly, account for the differences between [³H]pirenzepine and [³H]quinuclidinyl benzilate binding in rat cerebral cortex.

INTRODUCTION

The muscarinic receptor antagonist QNB³ binds with high affinity to an apparently homogeneous population

These studies were supported by United States Public Health Service Grants GM 31155 and BRSG S07-RR-05415-22.

¹ Recipient of National Institutes of Health Postdoctoral Fellowship F32-GM-09991.

² Established Investigator of the American Heart Association.

³ The abbreviations used are: QNB, quinuclidinyl benzilate; PZ, pirenzepine; L, ligand; R, receptor protein; LR*, isomerized form of a ligand-receptor complex; LR, ligand-receptor complex; $K_1 = k_{-1}/k_1$; $K_2 = k_{-2}/k_2$.

of binding sites in rat cerebral cortex (1, 2). It has been demonstrated more recently that, when the muscarinic antagonist PZ competes with [³H]QNB for binding sites in some brain regions, it distinguishes apparently heterogeneous binding sites (3, 4). [³H]PZ appears to bind to a single high-affinity muscarinic receptor site in brain, but it labels fewer sites than does [³H]QNB (4-6). These data, in combination with the ability of PZ and other muscarinic drugs to inhibit selectively certain physiological measures of muscarinic receptor activity (7, 8), have been interpreted to suggest heterogeneity of muscarinic receptor sites (7, 9).

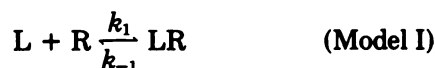
It has also been demonstrated that the binding of

0026-895X/84/050164-06\$02.00/0

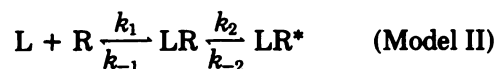
Copyright © 1984 by The American Society for Pharmacology and Experimental Therapeutics.

All rights of reproduction in any form reserved.

muscarinic receptor antagonists to cellular recognition sites may not conform to a simple bimolecular interaction of ligand with receptor:



For example, it has been proposed that antagonist binding to muscarinic receptors from atrium (10, 11) and smooth muscle (12) may proceed via a two-step mechanism:



This hypothesis was supported by kinetic data which demonstrated a nonlinear dependence of the pseudo-first-order association rate constant (k_{obs}) on ligand concentration (10–12). The data were consistent with a model for muscarinic ligand binding that had a rapid, initial binding interaction followed by a more slowly equilibrating reaction, yielding a complex with a different affinity state (13–15), such as Model II. It should be noted that these types of data are only consistent with Model II if LR dissociates rapidly (16), making LR unmeasurable under the conditions of the assay. Similar two-step binding interactions have been proposed for other receptor (17–19) and enzyme (13–15) systems.

Although detailed studies on muscarinic receptor isomerization have been performed in peripheral tissues, similar extensive studies have not been carried out with brain tissues. In addition, since [^3H]PZ appears to label fewer binding sites in the brain than does [^3H]QNB, we hypothesized that, if the [^3H]PZ-muscarinic receptor complex undergoes such an isomerization, this may explain the discrepancy between the observed density of [^3H]QNB and [^3H]PZ binding sites.

MATERIALS

[^3H]QNB was obtained from Amersham Corporation (Arlington Heights, Ill.) (38 Ci/mmol), or from New England Nuclear Corporation (Boston, Mass.) (33 Ci/mmol). [^3H]PZ (84 Ci/mmol) was obtained from New England Nuclear Corporation. Atropine sulfate, Tris, and oxotremorine sesquifumarate were from Sigma Chemical Company (St. Louis, Mo.), and PZ was a generous gift from Dr. R. Hammer, Thomae, Biberach an der Riss, Germany.

METHODS

Tissue preparation. Male Sprague-Dawley rats (200–250 g) were killed by decapitation, and the cerebral cortex from each rat was rapidly removed and placed into 4° buffer (10 mM Tris-HCl (pH 7.5) containing 1 mM EDTA). Tissue was homogenized at 4° using a 15-sec burst (setting of 6) on a Brinkmann Polytron. All subsequent operations were carried out at 4°. The homogenate was centrifuged at $20,000 \times g$ for 15 min, and the precipitated material thus obtained was resuspended in 20 mM Tris-HCl (pH 7.5) containing 0.9% NaCl.

Binding assay. Binding assays were performed as described previously (4), except that assays were performed at 25°. [^3H]QNB binding was determined by incubating tissue (approximately 20 μg of protein) with [^3H]QNB in a final volume of 5 ml. [^3H]PZ binding was determined in a final volume of 0.25 ml, containing approximately 0.4 mg of protein. Nonspecific binding for both ligands was defined as binding observed in the presence of 1 μM atropine and was always less than 50% of total binding. Reactions were terminated by addition of ice-cold wash buffer

(10 mM Tris-HCl/0.9% NaCl, pH 7.5) containing 1 μM atropine, followed immediately by filtration over glass-fiber filters (Schleicher and Schuell no. 30). Filters were rinsed immediately with 5 ml of the same wash buffer. Filters were then air-dried, and 4 ml of scintillation cocktail (Research Products International 2a70 (4 mg/ml) in 2:1 toluene/Triton X-100) were added. Samples were counted at an efficiency of approximately 32% for ^3H .

Data analysis. Experimental data were computer-fitted to models for ligand-receptor interactions described in the text, using the iterative public procedure FITFUN on the PROPHET system. Estimates of parameter values and their variances were obtained by least-squares regression analysis of untransformed data. Data are described as better “fit” by one model for ligand binding than another when a partial F -test (20) comparing the two models indicated a significant improvement in residual sum of squares ($p < 0.001$). The F -value for comparing two models was calculated from an analysis of residuals, according to the following equation:

$$F = \frac{\frac{SS_1 - SS_2}{df_1 - df_2}}{\frac{SS_2}{df_2}}$$

where SS_1 and SS_2 are residual sums of squares with corresponding degrees of freedom of df_1 and df_2 , associated with the simpler and more complex models, respectively. F -values were calculated using $df_1 - df_2$ degrees of freedom in the numerator and df_2 degrees of freedom in the denominator (20).

RESULTS

Determination of the number of binding sites for each radioligand. Saturation isotherms for the binding of [^3H]PZ and [^3H]QNB at equilibrium to cerebral cortical membranes are shown in Fig. 1. The saturation data for both ligands were consistent with simple bimolecular ligand-receptor interactions according to Model I. Scatchard replots of these data were linear (data not shown; cf. ref. 4). The receptor concentrations calculated from these and similar data were 0.97 ± 0.27 and 2.57 ± 0.68 pmol/mg of protein for [^3H]PZ and [^3H]QNB, respectively (Fig. 1). In this study, [^3H]PZ labeled 40% of the number of [^3H]QNB binding sites, and these results are in agreement with other data (4–6) which suggested that [^3H]PZ labeled fewer sites than did [^3H]QNB in rat cerebral cortex.

Rates of association of [^3H]PZ and [^3H]QNB at varying radioligand concentrations. The rates of association of [^3H]PZ and [^3H]QNB were determined at various concentrations of each of the ^3H -ligands. Initial experiments established that termination of binding assays using filtration alone, or by dilution with buffer containing no atropine, followed by filtration, was not rapid enough to permit characterization of early (e.g., < 0.5-min) time points in kinetic experiments. We therefore found that, under the latter assay conditions, significant binding was observed at zero time points, presumably by ligand-receptor association during the filtration process. Binding at time zero was reduced to undetectable levels when reactions were terminated with ice-cold buffer containing 1 μM atropine; for all routine assays of binding kinetics, atropine was therefore included to terminate radioligand-receptor interactions. Similarly, the assay temperature in the current experiments was reduced from 32°, as described in our previous study (4), to 25°. This was done

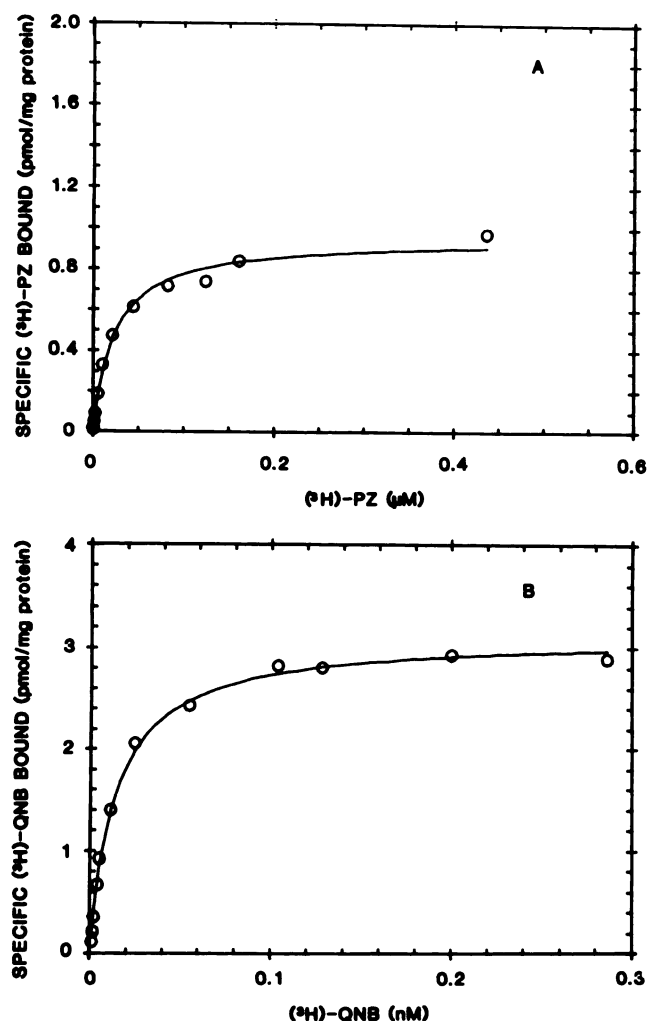


FIG. 1. Saturation analysis of [^3H]PZ and [^3H]QNB binding to cerebral cortical membranes at equilibrium

Specific [^3H]PZ and [^3H]QNB binding was determined following a 1-hr and a 6-hr incubation at 25° for [^3H]PZ and [^3H]QNB, respectively, as described under Methods. The curves shown were computer-modeled from the binding data, assuming binding of radioligand to a single class of noninteracting sites. Ligand concentrations represent total added ligand minus bound ligand.

A. [^3H]PZ binding. The K_d and B_{max} values for [^3H]PZ binding in this study were calculated to be 23 nM and 0.96 pmol/mg of protein, respectively. From these and similar data, the average density of [^3H]PZ binding sites was determined to be 0.97 ± 0.27 pmol/mg of protein (mean \pm standard deviation; $n = 6$).

B. [^3H]QNB binding. The K_d and B_{max} values for [^3H]QNB binding in this study were calculated to be 14 pM and 3.1 pmol/mg of protein, respectively. From these and similar data the average density of [^3H]QNB binding sites was determined to be 2.57 ± 0.68 pmol/mg of protein (mean \pm standard deviation; $n = 4$).

to permit a more accurate assessment of association rate constants, as ligand binding was extremely rapid at high ligand concentrations (see Fig. 2), even at 25°. Figure 2 shows pseudo-first-order replots (16) of the association data from representative experiments. The pseudo-first-order replots of data obtained at each ligand concentration were linear with respect to time (Fig. 2), and the pseudo-first-order rate constant of association (k_{obs}) at each ligand concentration was estimated using linear

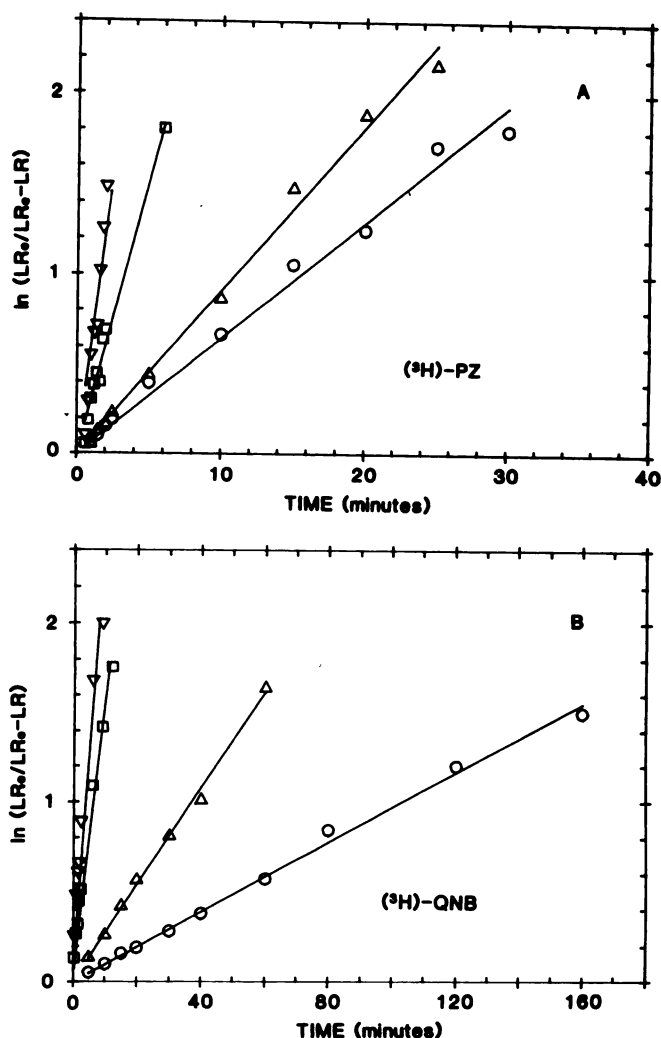


FIG. 2. Determination of the pseudo-first-order rate constant of association for [^3H]PZ and [^3H]QNB

[^3H]PZ and [^3H]QNB binding reactions were initiated (time zero) by the rapid combination of tissue and reaction mixture, which were separately prewarmed to 25°. Reactions were terminated by dilution with ice-cold buffer [10 mM Tris (pH 7.5)/0.9% NaCl] containing 1 μM atropine at the indicated time points, followed by rapid vacuum filtration, as described under Methods. The binding data obtained at each ligand concentration were plotted according to the equation:

$$\ln \frac{LR_0}{LR_0 - LR} = k_{\text{obs}} t$$

where LR_0 and LR are concentrations of radioligand specifically bound at equilibrium and at time t , respectively, and k_{obs} is the pseudo-first-order rate constant of association. Each point represents the mean of duplicate determinations from representative experiments. Values for k_{obs} were calculated from the slopes of the lines at each ligand concentration. For clarity, only four lines (of 14–18 determinations) are shown on each panel. A. [^3H]PZ: \circ , 1.21 nM; Δ , 6.46 nM; \square , 65.5 nM; ∇ , 168 nM. B. [^3H]QNB: \circ , 0.027 nM; Δ , 0.129 nM; \square , 2.54 nM; ∇ , 4.91 nM.

regression analysis to determine the slope of the lines. At high concentrations of ligands these lines appeared to approach a limiting slope.

Relationship of k_{obs} and radioligand concentration. Figure 3 demonstrates that plots of k_{obs} versus concentration deviated from linearity. According to Model I for ligand-

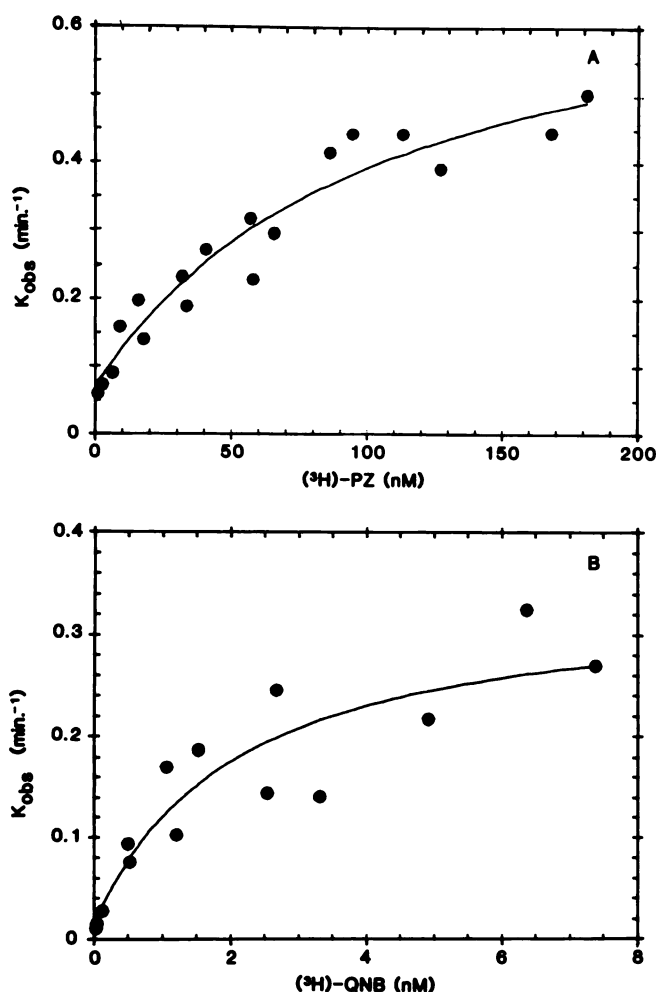


FIG. 3. Dependence of k_{obs} on $[^3H]PZ$ and $[^3H]QNB$ concentrations. Values for k_{obs} were determined as described in Fig. 2, using varying concentrations of $[^3H]PZ$ and $[^3H]QNB$, and the data from three such experiments were combined. The curves shown were computer-modeled with Eq. 1 to determine the values given in Table 1, as described in the text. Each point represents a determination of $k_{obs}(\text{min}^{-1})$ at one radioligand concentration. A. $[^3H]PZ$. B. $[^3H]QNB$.

receptor interaction, a linear relationship between k_{obs} and ligand concentration is predicted (16). As discussed by Strickland *et al.* (13) and others (12, 14, 15), the data in Fig. 3 are consistent with a two-step ligand receptor interaction (Model II) if (a) $k_{-1} \gg k_{-2}$ and (b) $k_{-1} \gg k_2$. Both of these conditions suggest that the isomerized form (LR^*) of the ligand-receptor complex is the only form of the receptor which would be recognized under our filtration binding assay conditions (12, 13, 15).

Rates of dissociation of $[^3H]PZ$ and $[^3H]QNB$: determination of k_{-2} . Model II predicts a hyperbolic relationship between k_{obs} and ligand concentration if LR^* is the only ligand-bound form of the receptor measured in the binding assay (12–15). The equation that describes this hyperbolic relationship has been discussed by Strickland *et al.* (13):

$$k_{obs} = \frac{k_2 (L)}{K_1 + (L)} + k_{-2} \quad (1)$$

If Model II correctly represents the molecular inter-

actions of $[^3H]PZ$ and $[^3H]QNB$ with cortical muscarinic receptors, and if LR^* is the only species measured in the binding assay, then the values of the observed dissociation rate constants determined for these radioligands (Fig. 4) represent estimates of k_{-2} . Exponential fits of the untransformed dissociation data were monophasic, and therefore the slopes of first-order replots of the dissociation data (Fig. 4) were used to estimate k_{-2} . The calculated values of k_{-2} were 0.07 and 0.0012 min^{-1} for $[^3H]PZ$ and $[^3H]QNB$, respectively. The values of k_{-2} for $[^3H]PZ$ and $[^3H]QNB$ were not different when either oxotremorine or PZ was used in place of atropine to initiate dissociation (data not shown). Because of the relatively long half-time of dissociation for $[^3H]QNB$, routine measurements of k_{-2} were made between 0 and 6 hr. After 21 hr, the rate of dissociation of $[^3H]QNB$ still appeared monophasic (data not shown), although after this prolonged incubation at 25° control binding was reduced by 25–30% and the calculation of percentage dissociation had to be corrected for this observation.

Computer modeling of the data in Fig. 3 to a straight line (i.e., Model I) and to Eq. 1 (i.e., Model II) suggested that the data were significantly better fit by Eq. 1 than by the straight line ($p < 0.001$). We concluded that the complex $[^3H]PZ$ and $[^3H]QNB$ binding kinetics could therefore be a consequence of an isomerization step, if the assumptions made regarding Model II were correct. Computer modeling of the data to Eq. 1 gave the estimated parameter values presented in Table 1, when values for k_{-2} were constrained during modeling to the

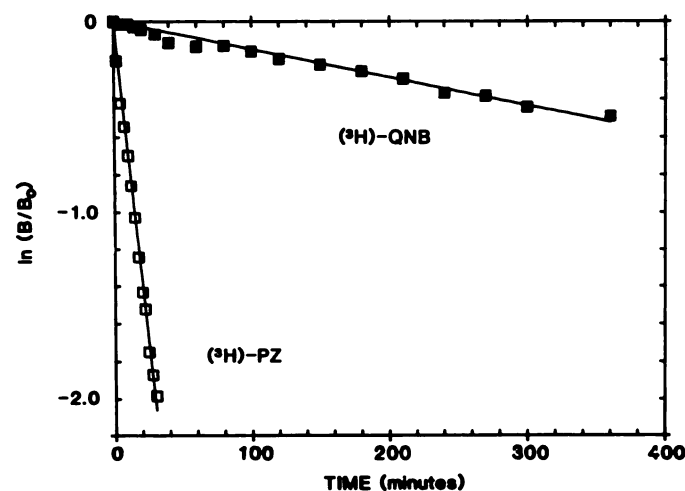


FIG. 4. Determination of k_{-2} for $[^3H]PZ$ and $[^3H]QNB$

Tissue was mixed and preincubated at 25° for 30 or 105 min with $[^3H]PZ$ or $[^3H]QNB$, respectively. Following the preincubation (time zero), 0.05 volume of atropine was added (final atropine = 1 μM), and specific binding was determined at the indicated time points, as described under Methods. Each point represents the mean of triplicate determinations in a single representative experiment. Data were replotted according to the following equation:

$$\ln\left(\frac{B}{B_0}\right) = k_{-2}t$$

where B_0 = specific radioligand binding at time zero and B = specific radioligand binding at time t (minutes). Values of k_{-2} (min^{-1}) for $[^3H]PZ$ and $[^3H]QNB$ were determined from the slopes of the lines. \square , $[^3H]PZ$ (12 nM); \blacksquare , $[^3H]QNB$ (250 pM).

TABLE 1

Constants for [³H]PZ and [³H]QNB binding calculated using Eq. 1

Parameter	Ligand	
	[³ H]PZ ^a	[³ H]QNB ^a
k_{-2} (min ⁻¹) ^b	0.070 ± 0.003 (3)	0.0012 ± 0.0003 (3)
k_2 (min ⁻¹) ^c	0.67 ± 0.10 (18)	0.322 ± 0.05 (14)
K_2 ^d	0.105	0.004
K_1 (nM) ^c	105 ± 30 (18)	1.61 ± 0.70 (14)
K_d (nM) ^d	11	0.006
%R _T ^e	90.5	99.6

^a Results shown are means ± standard deviation; the number of determinations is shown in parentheses.

^b Values for k_{-2} were obtained from the slopes of first-order replots of the dissociation rate data (Fig. 4).

^c Values for k_2 and K_1 were obtained by computer modeling the data shown in Figs. 3 and 4 to Eq. 1. The numbers in parentheses are the numbers of determinations of k_{obs} used in the modeling.

^d $K_2 = k_{-2}/k_2$; $K_d = K_1 \times K_2$.

^e The relative percentage of the total receptor concentration expected to be labeled by each radioligand using the filtration binding assay was calculated from Eq. 2.

experimentally determined (e.g., Fig. 4) values of 0.07 and 0.0012 min⁻¹ for [³H]PZ and [³H]QNB, respectively. The estimates of k_{-2} obtained when this parameter was not constrained in the computer modeling were indistinguishable from the experimentally determined values for [³H]PZ and [³H]QNB; however, confidence intervals (but not the parameter estimates themselves) for estimates of k_{-2} and K_1 (Eq. 1) were significantly reduced when these two parameters alone were estimated, rather than when k_2 was included as a third parameter in the modeling procedure.

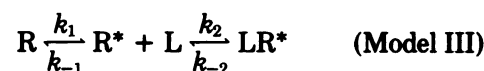
Values for K_2 and K_d in Table 1 were calculated as the ratio k_{-2}/k_2 and the product $K_1 \times K_2$, respectively. The values of K_d for [³H]PZ and [³H]QNB in Table 1 are in reasonable agreement with experimentally determined values (Fig. 1). Of particular interest in Table 1 are the values of K_2 , which predict that [³H]PZ and [³H]QNB would not label an identical number of sites in direct binding assays. While [³H]QNB would label >99% of the total receptor population with which it interacts, [³H]PZ would identify only approximately 90% of those receptors with which it interacts (see Eq. 2 under Discussion).

DISCUSSION

Several groups of investigators have suggested that binding of ligands to muscarinic cholinergic receptors obtained from heart (10, 11, 21), clonal cell lines (22), smooth muscle (12), and brain (12, 23) occurred via two-step mechanisms. These investigators have proposed an initial, rapidly equilibrating binding step that was followed by a more slowly equilibrating receptor isomerization step (10–12, 21–23; Model II). Two lines of evidence obtained in direct binding assays have been consistent with this hypothesis. Biphasic association and dissociation kinetics for muscarinic ligands have been observed in some studies (22, 23), whereas other studies have demonstrated a nonlinear dependence of the pseudo-first-order association rate constant on ligand concentration (10–12). Similar binding mechanisms have been proposed for the nicotinic cholinergic receptor in

electric organ (17–19) as well as several enzyme systems (13–15).

In this report, we have demonstrated using direct binding assays that the pseudo-first-order rate constant (k_{obs}) for ligand association with the muscarinic receptor in rat cerebral cortex exhibits a nonlinear dependence on ligand concentration. A linear dependence of k_{obs} on ligand concentration would be predicted by a simple binding interaction according to Model I, and also by Model II, if both LR and LR* were measured in the binding assay. Our results are not consistent with either of these latter possibilities. Our results are similarly not consistent with another possibility that the radioligand selectively binds to one of two pre-equilibrated species of R:



Model III predicts a hyperbolic dependence of k_{obs} on ligand concentration if only LR* is measured (i.e., $k_2 \gg k_1$ and $k_{-1} \gg k_{-2}$). However, Model II predicts (at low ligand concentrations) that k_{obs} would increase with ligand concentration, while Model III predicts that k_{obs} would decrease with increasing ligand concentration (13, 14), which it does not.

According to either Model I or Model II, saturation isotherms of equilibrium ligand binding would appear to conform to a simple mass-action interaction of ligand with receptor, if LR (Model I) and LR* (Model II) are the forms of ligand-bound receptor which are identified in the binding assays. However, in Model II, the value of the isomerization constant K_2 determines the fraction of receptors measured at saturating ligand concentrations; therefore, the observed density of receptors determined by saturation analysis (B_{max}^{obs}) will be a function of both the true density of receptors (B_{max}^{true}) and the value of K_2 :

$$B_{max}^{obs} = \frac{B_{max}^{true}}{(1 + K_2)} \quad (2)$$

Model II therefore predicts that, even though all Scatchard plots of binding data would be linear, a variable number of receptors (B_{max}) would appear to be labeled by different radioligands which exhibit different values of K_2 .

Our studies do not conclusively establish that Model II correctly describes the molecular interactions of [³H]PZ and [³H]QNB with muscarinic receptors. However, our kinetic studies were not consistent with binding Models I or III, but were consistent with Model II for both [³H]PZ and [³H]QNB binding to cerebral cortical membranes. The kinetic and equilibrium constants were therefore determined according to Model II for both ligands, by computer-modeling binding data to Eq. 1. If Model II correctly describes [³H]PZ and [³H]QNB binding, the relative distributions of the species LR and LR* would be dissimilar for [³H]PZ and [³H]QNB. It was calculated from Eq. 2 that, although >99% of the total receptor population would be in the form LR* using saturating concentrations of [³H]QNB, only approximately 90% would appear as LR* using saturating concentrations of [³H]PZ in equilibrium binding determi-

nations. These data predict that, if the true density of receptors (B_{\max}^{true}) for each ligand were equal, the observed maximal concentrations of [^3H]PZ binding sites (B_{\max}^{obs}) would appear to be 10% lower than concentrations of [^3H]QNB binding sites in cortex.

We have previously determined (4) that, under assay conditions similar to those used in this study, the density of [^3H]PZ binding sites was less than the density of [^3H]QNB binding sites in cerebral cortex. Indirect determinations of PZ binding suggested that there were high- and low-affinity components of PZ binding in rat cerebral cortex (3, 4), and that high-affinity PZ binding accounted for only a fraction of the total receptors which were labeled by [^3H]QNB. In this study, we demonstrated that [^3H]PZ labeled approximately 40% of the number of receptors labeled by [^3H]QNB (Fig. 1). Therefore, Model II cannot fully account for observed differences between [^3H]PZ and [^3H]QNB binding in cortex, but could account for approximately 10% of the difference. We interpret these data and previous data (3–6) to suggest that PZ may interact with a second, low-affinity binding site or coupling state of the muscarinic receptor which is not measurable in filtration binding assays using [^3H]PZ.

In summary, our data support the hypothesis that ligand-muscarinic receptor interactions in cerebral cortex are not simple (Model I), but instead may involve a two-step equilibrium (Model II). This is in agreement with several other studies in other tissues (10–12, 21–23). The kinetic and equilibrium parameters associated with Model II were determined for [^3H]PZ and [^3H]QNB. Although values for these parameters were not identical for both ligands, Model II cannot account for observed differences in the density of binding sites for [^3H]PZ and [^3H]QNB in cerebral cortex.

REFERENCES

1. Yamamura, H. I., and S. H. Snyder. Muscarinic cholinergic receptor binding in the longitudinal muscle of the guinea pig ileum with ^3H -quinuclidinyl benzilate. *Mol. Pharmacol.* 10:861–867 (1974).
2. Birdsall, N. J. M., E. C. Hulme, and A. S. V. Burgen. The character of the muscarinic receptors in different regions of the rat brain. *Proc. R. Soc. Lond. B Biol. Sci.* 207:1–12 (1980).
3. Hammer, R., C. P. Berrie, N. J. M. Birdsall, A. S. V. Burgen, and E. C. Hulme. Pirenzepine distinguishes between different subclasses of muscarinic receptors. *Nature (Lond.)* 283:90–92 (1980).
4. Luthin, G. R., and B. B. Wolfe. Comparison of ^3H -pirenzepine and ^3H -quinuclidinylbenzilate binding to muscarinic cholinergic receptors in rat brain. *J. Pharmacol. Exp. Ther.* 228:648–655 (1984).
5. Watson, M., W. R. Roeske, and H. I. Yamamura. ^3H -Pirenzepine selectively identifies a high-affinity population of muscarinic cholinergic receptors in the rat cerebral cortex. *Life Sci.* 31:2019–2023 (1982).
6. Watson, M., H. I. Yamamura, and W. R. Roeske. A unique regulatory profile and regional distribution of ^3H -pirenzepine binding in the rat provide evidence for distinct M_1 and M_2 muscarinic receptor subtypes. *Life Sci.* 32:3001–3011 (1983).
7. Hammer, R., and A. Giachetti. Muscarinic receptor subtypes: M_1 and M_2 biochemical and functional characterization. *Life Sci.* 31:2991–2998 (1983).
8. Hirschowitz, B. I., J. Fong, and E. Molina. The effects of pirenzepine and atropine on vagal and cholinergic gastric secretion and gastrin release and on heart rate in the dog. *J. Pharmacol. Exp. Ther.* 225:263–268 (1983).
9. Goyal, R. K., and S. Rattan. Neurohormonal, hormonal, and drug receptors for the lower esophageal sphincter. *Prog. Gastroenterol.* 74:598–619 (1978).
10. Shimerlik, M. I., and R. P. Searles. Ligand interactions with membrane-bound porcine atrial muscarinic receptor(s). *Biochemistry* 19:3407–3413 (1980).
11. Herron, G. S., S. Miller, W.-L. Manley, and M. I. Shimerlik. Ligand interactions with the solubilized porcine atrial muscarinic receptor. *Biochemistry* 21:515–520 (1982).
12. Jarv, J., B. Hedlund, and T. Bartfai. Isomerization of the muscarinic receptor-antagonist complex. *J. Biol. Chem.* 254:5595–5598 (1979).
13. Strickland, S., G. Palmer, and V. Massey. Determination of dissociation constants and specific rate constants of enzyme substrate (or protein-ligand) interactions from rapid reaction kinetic data. *J. Biol. Chem.* 250:4048–4052 (1975).
14. Hammes, G. G., and C.-W. Wu. Kinetics of allosteric enzymes. *Annu. Rev. Biophys. Bioeng.* 3:1–33 (1974).
15. Quast, U., J. Engel, H. Heumann, G. Kraube, and E. Steffen. Kinetics of the interaction of bovine pancreatic trypsin inhibitor (kunitz) with α -chymotrypsin. *Biochemistry* 13:2512–2520 (1974).
16. Weiland, G., and P. B. Molinoff. Quantitative analysis of drug-receptor interactions. I. Determination of kinetic and equilibrium properties. *Life Sci.* 29:313–330 (1981).
17. Quast, U., M. Shimerlik, T. Lee, V. Witzemann, S. Blanchard, and M. A. Raftery. Ligand-induced conformation changes in *Torpedo californica* membrane-bound acetylcholine receptor. *Biochemistry* 17:2405–2414 (1978).
18. Prinz, H., and A. Maelicke. Interaction of cholinergic ligands with the purified acetylcholine receptor protein. I. Equilibrium binding studies. *J. Biol. Chem.* 258:10263–10271 (1983).
19. Prinz, H., and A. Maelicke. Interaction of cholinergic ligands with the purified acetylcholine receptor protein. II. Kinetic studies. *J. Biol. Chem.* 258:10273–10282 (1983).
20. Hoyer, D., E. E. Reynolds, and P. B. Molinoff. Agonist-induced changes in the properties of β -adrenergic receptors on intact S49 lymphoma cells: time-dependent changes in the affinity of the receptor for agonists. *Mol. Pharmacol.* 25:209–218 (1984).
21. Galper, J. B., and T. W. Smith. Properties of muscarinic acetylcholine receptors in heart cell cultures. *Proc. Natl. Acad. Sci. U. S. A.* 75:5831–5835 (1978).
22. Klein, W. L. Multiple binding states of muscarinic acetylcholine receptors in membranes from neuroblastoma \times glioma hybrid cells. *Biochem. Biophys. Res. Commun.* 93:1058–1066 (1980).
23. Kloog, Y., and M. Sokolovsky. Studies on muscarinic acetylcholine receptors from mouse brain: characterization of the interaction with antagonists. *Brain Res.* 144:31–48 (1978).

Send reprint requests to: Dr. Gary R. Luthin, Department of Pharmacology, University of Pennsylvania School of Medicine/G3, Philadelphia, Pa. 19104.